Theory of huge thermoelectric effect based on a magnon drag mechanism: Application to thin-film Heusler alloy

Hiroyasu Matsuura,[1,*] Masao Ogata,[1,2] Takao Mori,[3,4] and Ernst Bauer[5]

[1]*Department of Physics, University of Tokyo, 7-3-1 Hongo, Bunkyo, Tokyo 113-0033, Japan*

[2]*Trans-scale Quantum Science Institute, University of Tokyo, Bunkyo-ku, Tokyo 113-0033, Japan*

[3]*International Center for Materials Nanoarchitectonics (WPI-MANA), National Institute for Materials Science, Tsukuba 305-0044, Japan*

[4]*Graduate School of Pure and Applied Sciences, University of Tsukuba, Tennodai 1-1-1, Tsukuba 305-8671, Japan*

[5]*Institute of Solid State Physics, Technische Universität Wien, A-1040 Vienna, Austria*

(Received 5 August 2021; accepted 1 December 2021; published 15 December 2021)

To understand the unexpectedly high thermoelectric performance observed in the thin-film Heusler alloy $Fe_2V_{0.8}W_{0.2}Al$, we study the magnon drag effect, generated by the tungsten-based impurity band, as a possible source of this enhancement, in analogy to the phonon drag observed in $FeSb_2$. Assuming that the thin-film Heusler alloy has a conduction band integrating with the impurity band, originated by the tungsten substitution, we derive the electrical conductivity L_{11} based on the self-consistent t-matrix approximation and the thermoelectric conductivity L_{12} due to magnon drag based on the linear response theory and estimate the temperature-dependent electrical resistivity, Seebeck coefficient, and power factor. Finally, we compare the theoretical results with the experimental results of the thin-film Heusler alloy to show that the origin of the exceptional thermoelectric properties is likely due to the magnon drag related to the tungsten-based impurity band.

DOI: 10.1103/PhysRevB.104.214421

I. INTRODUCTION

Thermoelectric materials have attracted much attention because they can directly convert thermal energy to electric energy [1–3]. Especially, the development of thermoelectric materials, utilizing magnetism, has been a focus, and many materials with high thermoelectric performance have been found [4–8]. The efficiency of the thermoelectric conversion is expressed by the figure of merit ZT, defined by $ZT \equiv S^2\sigma T/\kappa$, where S, σ, T, and κ are the Seebeck coefficient, electrical conductivity, temperature, and thermal conductivity, respectively. However, it is well known that ZT is usually much lower than unity because it is difficult to control these physical quantities independently.

Recently, it was found that a thin-film Heusler alloy, $Fe_2V_{0.8}W_{0.2}Al$, shows a huge ZT ($ZT \sim 5$) at $T \sim 350$ K, deriving from a huge power factor defined as $\mathrm{PF} \equiv S^2\sigma$ [9]. The origin of these huge ZT and PF is expected to be related to the anomalous temperature dependence of the electrical resistivity and the Seebeck coefficient because the electrical resistivity changes from a metallic behavior to a semiconducting behavior at $T \sim 350$ K, and the Seebeck coefficient has a peak structure with a huge value ($S \sim -500$ μV/K) around this temperature.

In a previous study, on the basis of the first-principles calculation, the origin of this huge Seebeck coefficient was suggested to be a result of the large mobility due to many Weyl points and a large logarithmic energy derivative of the electronic density of states near the Fermi energy [9]. On the other hand, it was also claimed [10] that the crystal structure assumed in Ref. [9] is different from the experimental one. Then, it was reported that a new alloy model suggested in Ref. [10] gives rise to only a Seebeck coefficient $S \sim 30$ μV/K at $T \sim 400$ K, which is much smaller than the experimental value. However, the actual alloy structures of $Fe_2V_{0.8}W_{0.2}Al$ has not been fully explored both theoretically and experimentally. Furthermore, a contribution of magnetism related to the thin-film Heusler alloy [9] to the Seebeck coefficient has not yet been taken into account. In addition to recent experimental reports revealing an enhancement of the Seebeck coefficient of various systems through magnetic interactions [4,6,8], it was recently experimentally demonstrated that spin fluctuation enhances the Seebeck coefficient of a doped itinerant ferromagnetic Fe_2VAl system [5].

The temperature dependences of the electrical resistivity and Seebeck coefficient observed in this thin-film Heusler alloy are very similar to those in $FeSb_2$: $FeSb_2$ shows a huge Seebeck coefficient at low temperatures ($T \sim 10$ K), and at the same temperature, the electrical resistivity changes its temperature dependence to the semiconducting behavior as the temperature decreases [11]. The origin of this huge Seebeck effect observed in $FeSb_2$ has been suggested to be caused by phonon drag, in which acoustic phonons couple with large effective mass electrons in an impurity band [12–14]. From the analogy with $FeSb_2$, the origin of the huge Seebeck effect observed in the thin-film Heusler alloy is supposed to be magnon drag related in the context of an impurity band and a conduction band with large effective electron masses.

*matsuura@hosi.phys.s.u-tokyo.ac.jp

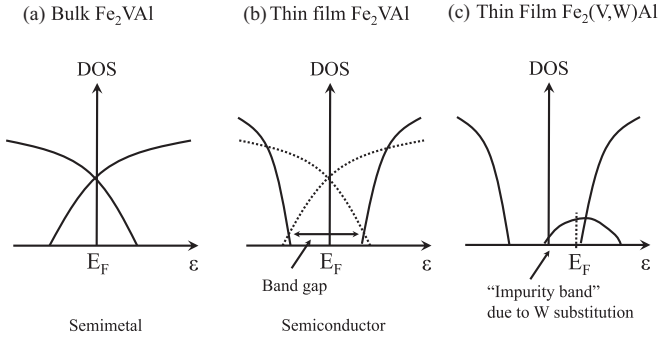

FIG. 1. Schematic pictures of the electronic states of (a) bulk Fe_2VAl, (b) thin-film Fe_2VAl, and (c) thin-film $Fe_2(V,W)Al$.

The contribution of the magnon drag to the Seebeck effect has been studied experimentally [15–18] and theoretically [19–23] from the 1960s. However, it appears that the magnon drag, related to an impurity band like in the present alloy, is not sufficiently understood.

In this paper, we study the magnon drag effect with an impurity state to clarify the origin of the huge Seebeck coefficient and PF observed in the thin-film Heusler alloy. First, since the electronic state of the thin-film Heusler alloy is not yet entirely understood, we assume an electronic state from the view point of a dimensional reduction. Extending the phonon drag theory studied in $FeSb_2$ [14] to the thin-film Heusler alloy, we study the temperature dependence of the electrical resistivity, Seebeck coefficient, and PF related to such an impurity state. We then compare the obtained theoretical results with experimental results to understand the origin of the huge thermoelectric effect observed in the thin-film Heusler alloy.

II. SCHEMATIC PICTURE OF ELECTRONIC STATES

First, we deduce the electronic state of the thin-film Heusler alloy based on the electronic state of bulk Fe_2VAl. Figure 1(a) shows a schematic picture of the electronic state of the bulk Fe_2VAl near the Fermi level. It is found [9,24,25] that this electronic state is a typical semimetallic state. In the thin film, it is expected that the bandwidth decreases due to the dimensional reduction. Therefore, we suggest that a band gap appears as a result of the lower dimension in the thin-film Fe_2VAl [Fig. 1(b)]. When vanadium is replaced by tungsten in this thin film, it is natural to expect impurity states to appear near the bottom of the conduction band because the energy level of $5d$ electrons in W is lower than the $3d$ energy level in V. Figure 1(c) shows a schematic picture of the electronic state of the thin-film Heusler alloy substituted by W. In this paper, we study the electrical and thermal transports on the basis of the electronic state shown in Fig. 1(c).

III. MODEL HAMILTONIAN AND FORMULATION OF ELECTRIC AND THERMAL TRANSPORTS

To study the magnon drag based on the electronic state shown in Fig. 1(c), we use the following model Hamiltonian [14,21–23]:

$$H = H_0 + H_{\rm W} + H_{\rm mag} + H_{\rm e-mag}, \tag{1}$$

where H_0, $H_{\rm W}$, $H_{\rm mag}$, and $H_{\rm e-mag}$ are Hamiltonians for the ferromagnetic conduction band, W sites, the ferromagnetic magnon, and the electron-magnon interaction, respectively. These Hamiltonians are given as $H_0 = \sum_{\mathbf{k},\sigma}(\epsilon_{\mathbf{k}\sigma} - \mu)c^\dagger_{\mathbf{k}\sigma}c_{\mathbf{k}\sigma}$, $H_W = V_0\sum_{\langle i\rangle} c^\dagger_{i\sigma}c_{i\sigma}$, $H_{\rm mag} = \sum_{\mathbf{q}}\hbar\omega_{\mathbf{q}}b^\dagger_{\mathbf{q}}b_{\mathbf{q}}$, and $H_{\rm e-mag} = \frac{I}{\sqrt{V}}\sum_{\mathbf{k},\mathbf{q}}[b^\dagger_{\mathbf{q}}c^\dagger_{\mathbf{k}\uparrow}c_{\mathbf{k}+\mathbf{q}\downarrow} + b_{\mathbf{q}}c^\dagger_{\mathbf{k}+\mathbf{q}\downarrow}c_{\mathbf{k}\uparrow}]$, where $c_{\mathbf{k}\sigma}$ or $c_{i\sigma}$ ($c^\dagger_{\mathbf{k}\sigma}$ or $c^\dagger_{i\sigma}$) is an annihilation (creation) operator of an electron with wave number $\mathbf{k}$ on the ith site and spin $\sigma = \uparrow\downarrow$ and $b_{\mathbf{q}}$ ($b^\dagger_{\mathbf{q}}$) is an annihilation (creation) operator of a magnon with wave vector $\mathbf{q}$. $\epsilon_{\mathbf{k}\sigma}$ is the energy dispersion in the ferromagnetic state, μ is the chemical potential, V_0 is the strength of a random impurity potential, $\langle i\rangle$ is the position of impurities, and $\hbar\omega_{\mathbf{q}}$ is the energy dispersion of ferromagnetic magnons, given by $\hbar\omega_{\mathbf{q}} = Dq^2$, where D is the spin wave stiffness constant. Finally, $I = J\sqrt{V}$ is the strength of the electron-magnon interaction, where J and V are the coupling constant between the electron and magnon and the volume of the unit cell, respectively. In this paper, we use the following simple energy dispersion: $\epsilon_{\mathbf{k}\uparrow} = \frac{\hbar^2k^2}{2m^*} - \Delta$ and $\epsilon_{\mathbf{k}\downarrow} = \frac{\hbar^2k^2}{2m^*}$, where m^* is the effective mass of conduction electrons and Δ is the energy difference between up-spin and down-spin electrons to express the ferromagnetic state, which corresponds to d orbitals of iron in $FeV_{0.8}W_{0.2}Al$ [9]. We assume that Δ is independent of temperature for simplicity. Because the Fermi energy is located near the bottom of the conduction band or in the impurity band, as shown in Fig. 1(c), the valence band is neglected, although it will contribute at high temperatures.

To treat the random potential of the W site, we use a self-consistent t-matrix approximation [14,26–29]. As discussed in Ref. [14], we define the retarded Green's function of an electron with spin σ as

$$G^R_\sigma(k,\epsilon) = \frac{1}{\epsilon - \epsilon_{\mathbf{k}\sigma} - \Sigma^R_\sigma(\epsilon)}, \tag{2}$$

where, by the self-consistent t-matrix approximation, the retarded self-energy $\Sigma^R_\sigma(\epsilon)$ is given as $\Sigma^R_\sigma(\epsilon) = \frac{n_iV_0}{1-\frac{V_0}{V}\sum'_{\mathbf{k}}G^R_\sigma(k',\epsilon)}$. Here, n_i is the concentration of W sites. The density of states (DOS) is obtained by $D_\sigma(\epsilon) = D_0{\rm Im}[y_\sigma]$, where $D_0 = \frac{\sqrt{(m^*)^3\epsilon_B}}{\sqrt{2}\pi^2\hbar^3}$ and y_σ is determined by solving the cubic equation: $y^3_\sigma - 2y_\sigma + (1 + \frac{\epsilon+\Delta\delta_{\sigma,\uparrow}}{\epsilon_B})y_\sigma - \nu = 0$ [14]. Here, $\nu \equiv 2\pi n_i\hbar^3/\sqrt{2(m^*)^3\epsilon^3_B}$. We assumed that ϵ_B ($\epsilon_B + \Delta$) is the binding energy of a single W impurity for down spin (up spin) as a first step. It should be noted that the first-principles calculation shows no spin splitting in $5d$ orbitals of W [9].

The Fermi energy E_F and the temperature dependence of the chemical potential are determined self-consistently by $\sum_\sigma\int^\infty_{-\infty} f(\epsilon)D_\sigma(\epsilon)d\epsilon = \sum_\sigma\int^{E_F}_{-\infty} D_\sigma(\epsilon)d\epsilon = n_i$, where $f(\epsilon)$ is the Fermi distribution function, defined as $f(\epsilon) = 1/(e^{\beta(\epsilon-\mu)} + 1)$.

The electrical current $\mathbf{J}_e$, the heat current due to electrons $\mathbf{J}^{\rm ele}_Q$, and the heat current due to ferromagnetic magnons $\mathbf{J}^{\rm mag}_Q$ are defined as $\mathbf{J}_e = e\sum_{\mathbf{k}\sigma} v_{\mathbf{k},\sigma}c^\dagger_{\mathbf{k},\sigma}c_{\mathbf{k},\sigma}$, $\mathbf{J}^{\rm ele}_Q = \sum_{\mathbf{k}\sigma}(\epsilon_{\mathbf{k}\sigma} -$

$\mu)v_{\mathbf{k},\sigma}c^{\dagger}_{\mathbf{k},\sigma}c_{\mathbf{k},\sigma}$, and $\mathbf{J}^{\rm mag}_{Q}=\sum_{\mathbf{q}}\hbar\omega_{\mathbf{q}}\frac{\partial\omega_{\mathbf{q}}}{\partial q_x}b^{\dagger}_{\mathbf{q}}b_{\mathbf{q}}$, where $v_{\mathbf{k},\sigma}=\frac{1}{\hbar}\frac{\partial\epsilon_{\mathbf{k},\sigma}}{\partial k_x}$ and e is the electron charge ($e<0$).

Under an electric field $\mathbf{E}$ and temperature gradient ∇T, the electrical current density $\mathbf{j}$ is described in the linear response theory as $\mathbf{j}=L_{11}\mathbf{E}+L_{12}(-\frac{\nabla T}{T})$, where L_{11} and L_{12} are electrical conductivity and thermoelectric conductivity, respectively [30]. These coefficients are calculated from the correlation function between the electrical currents and that between the electrical and heat currents derived by Kubo and Luttinger [31–33]:

$$L_{ij}=\lim_{\omega\to 0}\frac{\Phi_{ij}(\omega+i\delta)-\Phi_{ij}(0)}{i(\omega+i\delta)}, \tag{3}$$

where ω is the frequency of the external field. In the present case, L_{12} contains two components due to $J^{\rm ele}_{Q}$ and $J^{\rm mag}_{Q}$, which we refer to as $L^{\rm ele}_{12}$ and $L^{\rm drag}_{12}$, respectively.

The transport coefficient L_{11} due to the electrical currents and $L^{\rm ele}_{12}$ due to the electrical current and the heat current due to electrons are [33]

$$L_{11}=\int d\epsilon\left(-\frac{\partial f(\epsilon)}{\partial\epsilon}\right)\sigma(\epsilon), \tag{4}$$

$$L^{\rm ele}_{12}=\frac{1}{e}\int d\epsilon\left(-\frac{\partial f(\epsilon)}{\partial\epsilon}\right)(\epsilon-\mu)\sigma(\epsilon), \tag{5}$$

where $\sigma(\epsilon)$ is the function of electrical conductivity, depending on ϵ. The relaxation time of electrons is included in $\sigma(\epsilon)$. When we use the Green's function obtained in Eq. (2), $\sigma(\epsilon)$ is given by

$$\sigma(\epsilon)=\sum_{\sigma}\frac{e^2\sqrt{m^*}}{12\pi^2\hbar^2}\frac{[\sqrt{x_\sigma^2+\Gamma_\sigma(\epsilon)^2}+x_\sigma]^{\frac{3}{2}}}{\Gamma_\sigma(\epsilon)}, \tag{6}$$

where $x_\sigma=\epsilon+\Delta\delta_{\sigma,\uparrow}-{\rm Re}\Sigma^{\rm R}_{\sigma}(\epsilon)$ and $\Gamma_\sigma(\epsilon)=-{\rm Im}\Sigma^{\rm R}_{\sigma}(\epsilon)$, respectively. It has to be noted that we consider only the effect of the random potential, given by the self-consistent t-matrix approximation and neglect the effect of relaxation due to the electron-magnon interaction in the calculation of the electrical conductivity L_{11}.

Next, we study the correlation function between the electrical current and the heat current of magnons defined as $\Phi_{12}(\tau)=\frac{1}{V}\langle T_\tau[\mathbf{j}_e(\tau)\mathbf{j}^{\rm mag}_{Q}(0)]\rangle$, where τ is imaginary time and T_τ denotes the imaginary time ordering operator [22,23]. Using the second-order perturbation on the exchange interaction based on the Green's function of electrons, Eq. (2), the correlation function due to the magnon drag is obtained as

$$\Phi^{\rm drag}_{12}(\omega)=i\omega\frac{I^2e(m^*)^2}{48\pi^3\hbar^5\Gamma_{\rm mag}(T)}\int_0^{\epsilon_q^{\rm cut}}d\epsilon_q\frac{\beta\epsilon_q e^{\beta\epsilon_q}}{(e^{\beta\epsilon_q}-1)^2}$$
$$\times\int dx f(x)\left[\frac{L_1^+}{\Gamma_\downarrow(x+\epsilon_q)}-\frac{L_2^+}{\Gamma_\downarrow(x)}-\frac{L_1^-}{\Gamma_\uparrow(x)}+\frac{L_2^-}{\Gamma_\uparrow(x-\epsilon_q)}\right], \tag{7}$$

where $\Gamma_{\rm mag}(T)$ and $\epsilon_q^{\rm cut}$ are the temperature-dependent magnon relaxation rate and an energy cutoff of magnons, respectively; $L_1^{\pm}=\epsilon_q\pm\alpha\epsilon_q-\Delta-{\rm Re}\Sigma^{(\rm R)}_{\downarrow}(x+\epsilon_q)+{\rm Re}\Sigma^{(\rm R)}_{\uparrow}(x)$, and $L_2^{\pm}=\epsilon_q\pm\alpha\epsilon_q-\Delta+{\rm Re}\Sigma^{(\rm R)}_{\uparrow}(x-\epsilon_q)-{\rm Re}\Sigma^{(\rm R)}_{\downarrow}(x)$, where $\alpha=\frac{\hbar^2}{2m^*D}$. In the Supplemental Material, we show the derivation of Eq. (7) in detail [34]. Using Eq. (3), the thermoelectric conductivity due to the magnon drag $L^{\rm drag}_{12}$ is obtained. The vertex corrections, which are neglected in this paper for simplicity, were discussed in Ref. [23].

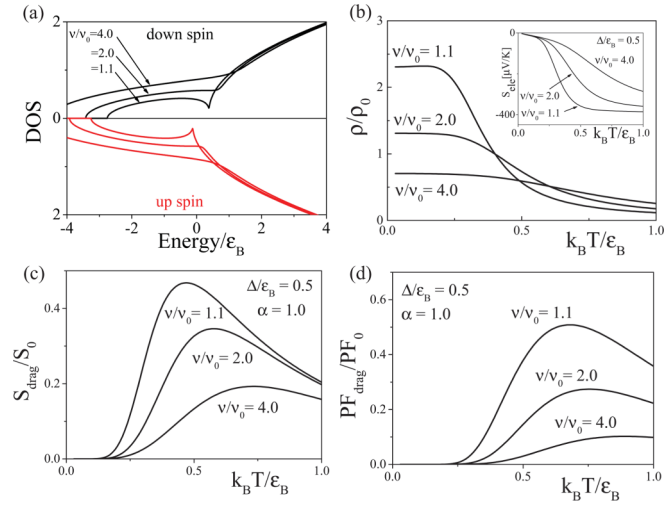

FIG. 2. (a) Density of states (DOS), (b) electrical resistivity, (c) the Seebeck coefficient due to the magnon drag $S_{\rm drag}$, and (d) the power factor due to the magnon drag $\rm PF_{drag}$ for $\tilde{\nu}\equiv\nu/\nu_0=1.1$, 2, and 4 and $\Delta/\epsilon_B=0.5$. The inset in (b) shows the Seebeck coefficient due to the heat current of the electron $S_{\rm ele}$.

IV. NUMERICAL RESULTS

Figure 2(a) shows the density of states for $\tilde{\nu}\equiv\nu/\nu_0=1.1$, 2, and 4. We set $\Delta/\epsilon_B=0.5$. For $\tilde{\nu}=2$ and 4, the impurity band hybridizes the conduction band naturally, while for $\tilde{\nu}=1.1$, the impurity band only slightly touches the conduction band. The Fermi energy is located in $E_F/\epsilon_B\simeq-1.20$ for $\tilde{\nu}=1.1$, -1.16 for $\tilde{\nu}=2$, and -1.07 for $\tilde{\nu}=4.0$. It should be noted that the chemical potential does not show a drastic temperature dependence.

Figure 2(b) shows the temperature-dependent electrical resistivity ($\rho=1/L_{11}$) for $\tilde{\nu}=1.1$, 2, and 4. Here, $\rho_0=12\pi^2\hbar^2/\gamma e^2\sqrt{m^*\epsilon_B}$. It has to be noted that we introduce the dimensionless phenomenological parameter γ to consider additional contributions of the valleys and other unspecified processes to the electrical conductivity. As shown in Fig. 2(b), the resistivity increases gradually, as the temperature decreases from high temperatures, while around $k_BT/\epsilon_B\simeq0.5$, the resistivity drastically increases; the resistivity becomes constant at low temperatures. This behavior is a result of the impurity band. We also conclude that the constant resistivity value at low temperatures depends on the impurity concentration.

Next, let us discuss the Seebeck coefficient due to the heat current of electrons, i.e., $S_{\rm ele}=L^{\rm ele}_{12}/TL_{11}$, and the Seebeck coefficient due to the magnon drag, i.e., $S_{\rm drag}=L^{\rm drag}_{12}/TL_{11}$. The inset of Figure 2(b) shows the temperature-dependent Seebeck coefficients $S_{\rm ele}$ for $\tilde{\nu}=1.1$, 2, and 4. As the impurity concentration decreases, the Seebeck coefficient increases, while the Seebeck coefficient does not show a peak structure. Figure 2(c) shows the temperature-dependent term $S_{\rm drag}$ for $\tilde{\nu}=1.1$, 2, and 4 and $\alpha=1.0$.

We assume a temperature-dependent magnon relaxation rate, $\Gamma_{\rm mag} = (\hbar/2\tau_0)T$, where τ_0 is a constant. The factor S_0 is defined by $S_0 = I^2(m^*)^{3/2}k_B^2\tau_0/2e\pi\hbar^4\sqrt{\epsilon_B}$. Note that the Seebeck coefficient does not depend on γ. As shown in Fig. 2(c), the Seebeck coefficient increases as the impurity concentration decreases. We also find that a peak structure of the temperature-dependent Seebeck coefficient appears around $k_BT/\epsilon_B \simeq 0.5$ for $\nu/\nu_0 = 1.1$, 0.6 for $\nu/\nu_0 = 2$, and 0.7 for $\nu/\nu_0 = 4$. Figure 2(d) shows the temperature-dependent power factor due to the magnon drag $\mathrm{PF}_{\rm drag}$, where we define $\mathrm{PF}_0 = S_0^2/\rho_0$. $\mathrm{PF}_{\rm drag}$ traces closely the temperature-dependent Seebeck coefficient shown in Fig. 2(c) for several impurity concentrations, while we find that the peak temperature of $\mathrm{PF}_{\rm drag}$ is higher than that of the Seebeck coefficient because of the distinct decrease in the electrical resistivity. It should be noted that the temperature dependences of $S_{\rm drag}$ and $\mathrm{PF}_{\rm drag}$ are insensitive to α, while these values strongly depend on α (see the Supplemental Material [34]).

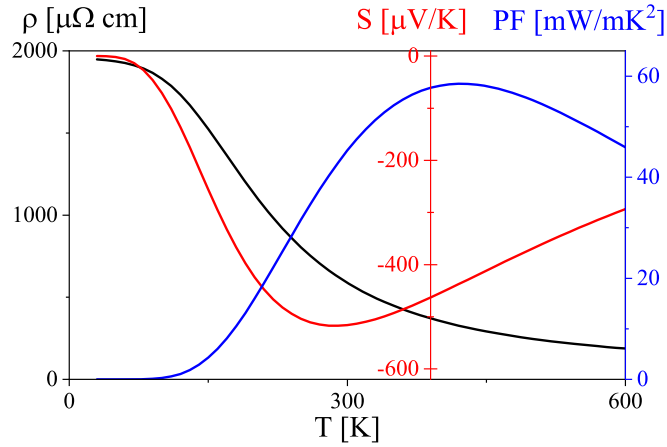

FIG. 3. Temperature dependences of the electrical resistivity, Seebeck coefficient due to the magnon drag, and power factor (PF) for realistic parameters.

V. DISCUSSION: COMPARISON WITH EXPERIMENTS

Here, we compare the obtained theoretical results with the experimental results for the thin-film Heusler alloy. Since there are no experimental data for theoretical parameters, we have chosen a set of the reasonable values: $\epsilon_B/k_B = 300$ K, $m^*/m_0 = 10$, $J/k_B = 1000$ K, $V = 10^{-27}$ m^3, and $\gamma = 10$. It should be noted that the large effective mass is due to the large density of states of the conduction band, as shown by the first-principles density functional theory calculations [9]; then, the impurity concentration n_i is of the order of 10^{27} m^{-3} for $\tilde{\nu} = 1$–4, which is consistent with the concentration of W in Fe_2VAl. Here, we set the lifetime of the magnon as $\tau = \tau_0/T \sim 10^{-14}$ s at $T = 300$ K. This value is reasonable for a ferromagnetic metal [35].

Using the parameters, $\nu/\nu_0 = 4$, and $\alpha = 1.0$, the temperature-dependent electrical resistivity and Seebeck coefficient due to the magnon drag, as well as the power factor, are displayed in Fig. 3. We find that the electrical resistivity attains $\rho \simeq 1000\ \mu\Omega$ cm at $T \sim 300$ K; we also find that the Seebeck coefficient due to the magnon drag exhibits a peak structure, with $S_{\rm max} \sim -500\ \mu$V/K at $T \sim 300$ K. The power factor reaches PF ~ 60 mW/m K^2 around $T \sim 400$ K. Since these theoretical results are similar to the experimental results, we presume that the origin of the huge Seebeck coefficient and the large PF observed experimentally for the thin-film Heusler alloy is likely due to magnon drag, related to the tungsten-based impurity band.

Finally, we comment on the lifetime of magnons. In this paper, we used a simple temperature-dependent lifetime for magnons. However, the lifetime is expected to be very complicated in a real material because it is derived from many kinds of scattering mechanisms such as impurity scattering, magnon-electron, magnon-magnon, and magnon-phonon interactions with or without the umklapp process, and so on. The understanding of these microscopic mechanisms for the lifetime of a magnon is a future problem.

VI. CONCLUSION

We studied the origin of the large Seebeck coefficient and unprecedented large PF observed in the thin-film Heusler alloy $FeV_{0.8}W_{0.2}Al$ on the basis of the linear response theory. Assuming that this thin-film alloy has a conduction band integrating with the impurity band originating from the W substitution and by extending the microscopic phonon drag theory observed in $FeSb_2$, we derived L_{11} based on the self-consistent t-matrix approximation and L_{12} due to the magnon drag. As a result, we found that the theoretical results of the Seebeck coefficient and PF are in agreement with the experimental ones. Therefore, we conclude that the origin of these striking thermoelectric properties is likely due to the magnon drag related to the W-based impurity band.

ACKNOWLEDGMENTS

This work is supported by Grants-in-Aid for Scientific Research from the Japan Society for the Promotion of Science (Grants No. JP18H01162, No. JP18K03482, and No. JP20K03802) and a JST-Mirai Program Grant (Grant No. JPMJMI19A1).

[1] L. E. Bell, Science **321**, 1457 (2008).
[2] K. Koumoto and T. Mori, *Thermoelectric Nanomaterials*, Springer Series in Materials Science Vol. 182 (Springer, Berlin, 2013).
[3] I. Petsagkourakis, K. Tybrandt, X. Crispin, I. Ohkubo, N. Satoh, and T. Mori, Sci. Tech. Adv. Mater. **19**, 836 (2018).
[4] A. Fahim, N. Tsujii, and T. Mori, J. Mater. Chem. A **5**, 7545 (2017).
[5] N. Tsujii, A. Nishide, J. Hayakawa, and T. Mori, Sci. Adv. **5**, eaat5935 (2019).
[6] S. Acharya, S. Anwar, T. Mori, and A. Soni, J. Mater. Chem. C **6**, 6489 (2018).

[7] Y. Zheng, T. Lu, Md M. H. Polash, M. Rasoulianboroujeni, N. Liu, M. E. Manley, Y. Deng, P. J. Sun, X. L. Chen, R. P. Hermann, D. Vashaee, J. P. Heremans, and H. Zhao, Sci. Adv. **5**, eaat9461 (2019).
[8] J. B. Vaney, S. A. Yamini, H. Takaki, K. Kobayashi, N. Kobayashi, and T. Mori, Mater. Today Phys. **9**, 100090 (2019).
[9] B. Hinterleitner, I. Knapp, M. Poneder, Y. Shi, H. Müller, G. Eguchi, C. Eisenmenger-Sittner, M. Stöger-Pollach, Y. Kakefuda, N. Kawamoto, Q. Guo, T. Baba, T. Mori, S. Ullah, X.-Q. Chen, and E. B. Bauer, Nature (London) **576**, 85 (2019).
[10] E. Alleno, A. Berche, J.-C. Crivello, A. Diack-Rasselio, and P. Jund, Phys. Chem. Chem. Phys. **22**, 22549 (2020).
[11] A. Bentien, S. Johnsen, G. K. H. Madsen, B. B. Iversen, and F. Steglich, Europhys. Lett. **80**, 17008 (2007).
[12] M. Battiato, J. M. Tomczak, Z. Zhong, and K. Held, Phys. Rev. Lett. **114**, 236603 (2015).
[13] H. Takahashi, R. Okazaki, S. Ishiwata, H. Taniguchi, A. Okutani, M. Hagiwara, and I. Terasaki, Nat. Commun. **7**, 12732 (2016).
[14] H. Matsuura, H. Maebashi, M. Ogata, and H. Fukuyama, J. Phys. Soc. Jpn. **88**, 074601 (2019).
[15] F. J. Blatt, D. J. Flood, V. Rowe, P. A. Schroeder, and J. E. Cox, Phys. Rev. Lett. **18**, 395 (1967).
[16] A. L. Trego and A. R. Mackintosh, Phys. Rev. **166**, 495 (1968).
[17] G. N. Grannemann and L. Berger, Phys. Rev. B **13**, 2072 (1976).
[18] S. J. Watzman, R. A. Duine, Y. Tserkovnyak, S. R. Boona, H. Jin, A. Prakash, Y. Zheng, and J. P. Heremans, Phys. Rev. B **94**, 144407 (2016).
[19] M. Bailyn, Phys. Rev. **126**, 2040 (1962).
[20] K. Sugihara, J. Phys. Chem. Solids **33**, 1365 (1972).
[21] D. Miura and A. Sakuma, J. Phys. Soc. Jpn. **81**, 113602 (2012).
[22] Y. Imai and H. Kohno, J. Phys. Soc. Jpn. **87**, 073709 (2018).
[23] T. Yamaguchi, H. Kohno, and R. A. Duine, Phys. Rev. B **99**, 094425 (2019).
[24] D. J. Singh and I. I. Mazin, Phys. Rev. B **57**, 14352 (1998).
[25] R. Weht and W. E. Pickett, Phys. Rev. B **58**, 6855 (1998).
[26] M. Saitoh, H. Fukuyama, Y. Uemura, and H. Shiba, J. Phys. Soc. Jpn. **27**, 26 (1969).
[27] T. Yamamoto and H. Fukuyama, J. Phys. Soc. Jpn. **87**, 024707 (2018).
[28] M. Ogata and H. Fukuyama, J. Phys. Soc. Jpn. **86**, 094703 (2017).
[29] M. Matsubara, K. Sasaoka, T. Yamamoto, and H. Fukuyama, J. Phys. Soc. Jpn. **90**, 044702 (2021).
[30] K. Behnia, *Fundamentals of Thermoelectricity*, (Oxford University Press, Oxford, 2015).
[31] R. Kubo, J. Phys. Soc. Jpn. **12**, 570 (1957).
[32] J. M. Luttinger, Phys. Rev. **135**, A1505 (1964).
[33] M. Ogata and H. Fukuyama, J. Phys. Soc. Jpn. **88**, 074703 (2019).
[34] See Supplemental Material at http://link.aps.org/supplemental/10.1103/PhysRevB.104.214421 for the derivation of Eq. (7) and α dependence of S_{drag} and PF_{drag}.
[35] Y. Zhang, T.-H. Chuang, Kh. Zakeri, and J. Kirschner, Phys. Rev. Lett. **109**, 087203 (2012).